

The Hamburg/SAO Survey for low metallicity blue compact/H II galaxies (HSS–LM).

I. The first list of 46 strong-lined galaxies

A.V. Ugryumov^{1,4}, D. Engels², S.A. Pustilnik^{1,4}, A.Y. Kniazev^{1,3,4}, A.G. Pramskij^{1,4}, and H.-J. Hagen²

¹ Special Astrophysical Observatory RAS, Nizhnij Arkhyz, Karachai-Circassia, 369167 Russia

² Hamburger Sternwarte, Gojenbergsweg 112, 21029 Hamburg, Germany

³ Max Planck Institut für Astronomie, Königstuhl 17, D-69117, Heidelberg, Germany

⁴ Isaac Newton Institute of Chile, SAO Branch

Received January 27, 2002; accepted September 16, 2002

Abstract. We present the description and the first results of a new project devoted to the search for extremely metal-deficient blue compact/H II-galaxies (BCGs) and to the creation of a well selected large BCG sample with strong emission lines.* Such galaxies should be suitable for reliable determination of their oxygen abundance through the measurement of the faint [O III] $\lambda 4363$ Å line. The goals of the project are two-fold: a) to discover a significant number of new extremely metal-poor galaxies ($Z \lesssim 1/20 Z_{\odot}$), and b) to study the metallicity distribution of local BCGs. Selection of candidates for follow-up slit spectroscopy is performed on the database of objective prism spectra of the Hamburg Quasar Survey. The sky region is limited by $\delta \geq 0^{\circ}$ and $b^{\text{II}} \leq -30^{\circ}$. In this paper we present the results of the follow-up spectroscopy conducted with the Russian 6 m telescope. The list of observed candidates contained 52 objects, of which 46 were confirmed as strong-lined BCGs ($EW([\text{O III}] \lambda 5007) \geq 100$ Å). The remaining five lower excitation ELGs include three BCGs, and two galaxies classified as SBN (Starburst Nucleus) and DANS (Dwarf Amorphous Nucleus Starburst). One object is identified as a quasar with a strong Ly α emission line near $\lambda 5000$ Å ($z \sim 3$). We provide a list with coordinates, measured radial velocities, B -magnitudes, equivalent widths $EW([\text{O III}] \lambda 5007)$ and $EW(\text{H}\beta)$ and for the 46 strong-lined BCGs the derived oxygen abundances $12+\log(\text{O}/\text{H})$. The abundances range between 7.42 and 8.4 (corresponding to metallicities between 1/30 and 1/3 Z_{\odot}). The sample contains four galaxies with $Z \lesssim 1/20 Z_{\odot}$, of which three are new discoveries. This demonstrates the high efficiency of the new project to find extremely metal-deficient galaxies. The radial velocities of the strong-lined ELGs range between 500 and 19000 km s⁻¹ with a median value of ~ 6400 km s⁻¹. The typical B -magnitudes of the galaxies presented are 17^m0 – 18^m0.

Key words. galaxies: blue compact – galaxies: abundances – galaxies: redshifts – galaxies: surveys

1. Introduction

Blue compact/H II galaxies (BCGs) are low-mass gas-rich objects which currently undergo an episode of enhanced star formation. Such episodes are usually recognized by a strong emission-line spectrum of H II type. Their duration is relatively short: strong emission lines are detectable on timescales from ten to a hundred Myr. These episodes of intense star formation are often called starbursts. BCGs are intensively studied since the seminal work by Sargent & Searle (1970), and especially actively during the last decade. The list of publications on this subject is very long, and we list below only those studies dealing with

observations and/or analysis of sufficiently large samples. These papers, among others, are Campos-Aguilar et al. (1993), Masegosa et al. (1994), Izotov et al. (1994), Thuan et al. (1995), Salzer et al. (1995), Pustilnik et al. (1995), Taylor et al. (1995), Vilchez (1995), Stasinska & Leitherer (1996), Telles & Terlevich (1997), van Zee et al. (1998a), Schaerer et al. (1997, 1999), Izotov & Thuan (1999), Bergvall et al. (1999), Thuan et al. (1999a), Kunth & Östlin (2000), Pustilnik et al. (2001b), and Ugryumov et al. (2001, and references therein).

To date more than thousand galaxies of this type are known. Part of them were found in early studies as Zwicky compact galaxies (Zwicky 1966) or Haro blue galaxies (Haro 1956). However, the great majority of BCGs were picked up by objective prism surveys such as the First and Second Byurakan (FBS, SBS) (Markarian 1967;

Send offprint requests to: A.V.Ugryumov, e-mail: and@sao.ru

* Figures A1–A6 are only available in the electronic form via <http://www.edpsciences.org>

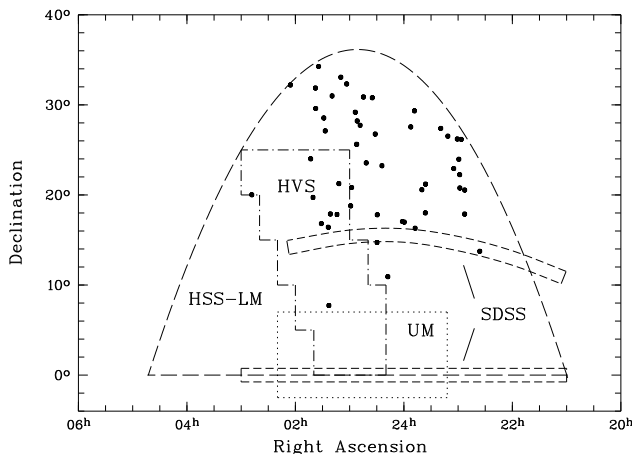


Fig. 1. The sky area covered by the HSS-LM is determined by $b^{II} \leq -30^\circ$ and $\delta \geq 0^\circ$. The positions of ELGs presented in this paper are shown with filled circles. The zones of three other surveys: University of Michigan (UM), Heidelberg void survey (HVS) and Sloan Digital Spectral Survey (SDSS) are shown as superimposed on the HSS-LM region (see references in the text).

Markarian et al. 1983; Stepanian 1994), the University of Michigan (Salzer et al. 1989b), the Tololo (Terlevich et al. 1991), the Case (Pesch et al. 1995; Salzer et al. 1995; Ugryumov et al. 1998), the Heidelberg void (Popescu et al. 1998) and the Hamburg/SAO survey (Ugryumov et al. 2001, and references therein).

Like other low-mass galaxies, BCGs have metallicities Z many times lower than those of normal bright galaxies. Their characteristic range of metallicity Z is $\sim (1/15 - 1/3) Z_\odot$ (e.g., Terlevich et al. 1991, Izotov et al. 1993), while very few of them show Z as low as $(1/50 - 1/20) Z_\odot$. All well studied BCGs with characteristic metallicities were found to be old galaxies, which evolve slower than their massive counterparts. Instead of having a lower gas consumption rate it was discussed during many years that galactic winds were responsible for a significant loss of heavy elements (Mac Low & Ferrara 1999), however more recent models (Silich & Tenorio-Tagle 2001, Legrand et al. 2002) indicate that for the majority of BCGs a significant loss of metals is rather improbable. In contrast to all typical BCGs a few well studied BCGs with an extreme deficit of heavy elements show properties of young galaxies, undergoing their first SF episode. In particular, they have gas-mass fractions (that is gas mass relative to all visible baryon mass) of the order 0.9–0.99 (e.g., Salzer et al. 1991, Kniazev et al. 2000b, Pustilnik et al. 2001a) and in the outermost parts of their low-surface brightness disks very blue colours, consistent with ages of the “old” stellar population less than 100–200 Myr.

One of the most often discussed candidate objects for a low age is I Zw 18 with $Z = 1/50 Z_\odot$, discovered by Searle & Sargent (1972). The most recent data are summarized by Izotov & Thuan (1999), Papaderos et al. (2002), van Zee et al. (1998b), Aloisi et al. (1999), and Östlin (2000).

While the first two papers forward arguments for a maximum age of less 200 Myr, Aloisi et al. (1999) and Östlin (2000) suggest an age of at least 1 Gyr. The age of the extremely metal poor galaxies remains therefore a hot matter of debate.

Several other well known objects are SBS 0335–052 (E and W) with $Z = 1/42 Z_\odot$ and $1/50 Z_\odot$ (e.g., Izotov et al. 1997; Papaderos et al. 1998; Lipovetsky et al. 1999; Pustilnik et al. 2001a, Östlin & Kunth 2001), HS 0822+3542 with $Z = 1/30 Z_\odot$ (e.g., Kniazev et al. 2000b; Pustilnik et al. 2002b; Izotov et al. 2002), Tol 1227–273 with $Z = 1/28 Z_\odot$ (e.g., Fricke et al. 2001) and CG 389 (1415+437) with $Z = 1/22 Z_\odot$ (e.g., Thuan et al. 1999b).

Most of the evidences is still indirect and in many cases controversial, but the study of these rare galaxies clearly stimulates our understanding of the earliest periods of galaxy evolution. Probably, these extremely metal-deficient BCGs are the best approximation of low-mass young galaxies expected to form commonly at redshifts $3 < z < 5$.

Despite 30 years of observations and more than a thousand known BCG galaxies, another important aspect of BCG studies remains unclear. What is the true metallicity distribution of BCGs and their progenitors? This has important cosmological implication, because the knowledge of the contemporary Z distribution allows to pose the question on their chemical evolution during the last few Gyr.

The results of BCG morphological studies indicate that they do not comprise a homogeneous group, but rather are a mixture of various types (e.g. Kunth et al. 1988; Doublier et al. 1997). This implies that BCG progenitors probably are not the rare type of gas-rich low-mass galaxies (see however, Salzer & Norton 1999). On the other hand, the recent results by Mouri & Taniguchi (2000), based on far-IR tracers of recent SF, indicate that up to $\sim (30 - 40)\%$ of the galaxies in their magnitude-limited sample within the galactic neighborhood have experienced SF activity during the last 100 Myr. The evidence that such a large fraction of galaxies experience episodes of significantly enhanced SF emphasizes the importance of BCG studies. In particular, the study of galaxies in the BCG phase allows easier to understand some of their progenitor parameters (such as Z), which are difficult to determine in more quiet periods of galaxy evolution.

Based on a large well selected sample of BCGs and using the model predictions for the evolution of observable parameters, such as $EW(H\beta)$, we hope to advance in restoring the true metallicity distribution of BCGs. This would be a major step to obtain the true Z -distribution of the BCG parent population – gas-rich low-mass galaxies.

These ideas are the motivation of our new project, “The Hamburg/SAO survey for low metallicity BCG/H II galaxies”. The sky region covered is limited by the southern galactic hemisphere north of $\delta = 0^\circ$ and $b^{II} \leq -30^\circ$. This large section of the sky is not well covered by spectroscopic surveys of sufficient depth. Besides of the First

Byurakan Survey (Markarian 1967) dealing with relatively bright galaxies, of a 9.5° wide strip of the University of Michigan (UM) Survey (MacAlpine et al. 1977; Salzer et al. 1989b and references therein) and of several fields of the Heidelberg void survey (HVS) (Hopp & Kuhn 1995; Popescu et al. 1996) there were no large deep surveys in this region. It will be covered in the nearest future by two 1.5° wide strips of the SDSS, having good spectroscopy for all galaxies brighter than $B \sim 18^m5$ (York et al. 2000), and in the more distant future this region will be covered by the 6dF-z project (Mamon 1999). The latter will obtain spectra only for relatively bright galaxies selected in the near-IR corresponding to $B \lesssim 16^m0$ for blue galaxies and hence will not compete with our significantly deeper survey. Therefore, most of the results obtained in the frame of this new survey will be valuable material for studies of strong-lined BCGs/H II galaxies in this region.

This project has several features in common to the earlier “Hamburg/SAO survey for emission-line galaxies” (HSS for ELGs), presented in a series of papers by Ugryumov et al. (1999) (I), Pustilnik et al. (1999) (II), Hopp et al. (2000) (III), Kniazev et al. (2001) (IV), Ugryumov et al. (2001) (V) and Pustilnik et al. (2002c) (VI).

The new project we will abbreviate as “HSS-LM” (LM — for low metallicity) to distinguish it from the “HSS” (for ELGs). The selection procedure used in the HSS is described in detail by Ugryumov et al. (1999). The main difference introduced in the HSS-LM is a more strict criterion on the strength of emission-line features in the full-resolution objective prism spectra. We select for follow-up long-slit spectroscopy only candidate galaxies with the strongest emission feature near $\lambda 5000 \text{ \AA}$, which, according to our previous experience, corresponds to the $[\text{O III}] \lambda 5007$ line with equivalent widths $EW > 150 - 200 \text{ \AA}$. Such galaxies are quite rare and their prism spectra are prominent enough not to miss them. Our slit spectroscopy justifies the correctness of the elaborated criterion. The great majority of the galaxies observed indeed have $EW([\text{O III}] \lambda 5007) > 150 \text{ \AA}$, and the fraction of galaxies with $EW([\text{O III}] \lambda 5007) < 100 \text{ \AA}$ is low (see Fig. 4).

The main advantage of this sample is that for most of these faint candidates the 6 m telescope spectra with moderate integration times ($\sim 20 \text{ min.}$) give a well detected $[\text{O III}] \lambda 4363 \text{ \AA}$ line, allowing the reliable determination of oxygen abundance by the standard method (Pagel et al. 1992).

In the context of an instantaneous SF burst the imposed selection criterion selects galaxies with very young SF bursts: typically younger than $5 - 10 \text{ Myr}$ (Schaerer & Vacca 1998; Leitherer et al. 1999). However, recent results indicate that quite often SF in BCGs proceeds in a more complicated mode, similar to a propagating wave of SF along the galaxy body (e.g., Zenina et al. 1997; Thuan et al. 2000 among others). Probably in this case, lines with large $EW([\text{O III}] \lambda 5007)$ come from regions close to the front of such a propagating SF wave.

In this paper we present the general outline of the project, give the details of the selection procedure and present the first list of galaxies observed spectroscopically. In Section 2 the selection criteria are discussed. In Section 3 the follow-up spectral observations and the data reduction are described. We present **some** results of the spectrophotometric observations and a brief summary in Section 4. The efficiency of this survey in detecting strong-lined ELGs and its perspectives are discussed and the respective conclusions are drawn in Section 5. Throughout the paper a Hubble constant of $H_0 = 75 \text{ km s}^{-1} \text{ Mpc}^{-1}$ is used.

2. Sample selection

The objects presented in this paper were selected from the digitized objective prism plates of the Hamburg Quasar Survey (Hagen et al. 1995).

2.1. Overview of the HSS selection

The original selection procedure used in the HSS was described in detail by Ugryumov et al. (1999), and some improvements were added in Kniazev et al. (2001). The HSS selection procedure picked up efficiently H II-galaxies with $EW([\text{O III}] \lambda 5007) > 50 \text{ \AA}$. It was optimized to deal with a large number of spectra ($30\,000 - 50\,000$ per plate) and aimed to reach a balance between a good completeness and a sufficiently high surface density in order to allow a study of their large-scale spatial distribution.

This procedure consisted of several steps. The first step was performed on the prism spectra digitized with low resolution (LRS). It allowed to discard more than $2/3$ of all spectra, which fall outside the predetermined region in the two-parameter (“slope”, “density”) space for LRS spectra. In the next step all preselected LRS were checked on a graphic screen to pick up the candidates with hints for $[\text{O III}] \lambda 5007 \text{ \AA}$ emission in order to reduce the number of candidates down to $3000 - 5000$. This number of LRS was sufficiently small to rescan them with the Hamburg PDS 1010 G microdensitometer in a high-resolution mode in order to get a confident selection of ELGs for follow-up spectroscopy.

2.2. Selection of HSS-LM candidates from the HQS database

In case of the HSS-LM the selection procedure adopted for the HSS was changed in order to speed up the selection and to increase the efficiency of the follow-up spectroscopy. The reason for this change are the different goals of the HSS-LM in comparison to those of the HSS. The former is intended to collect in a reasonable time a large sample of strong-lined ELGs with a well defined selection function and $EW([\text{O III}] \lambda 5007) > 150 - 200 \text{ \AA}$, among which we expect to find about half a dozen new extremely metal-deficient BCGs.

Table 1. Journal of observations at the SAO 6 m telescope

Run No (1)	Date (2)		Instrument (3)		Grating [grooves mm ⁻¹] (4)	Wavelength Range [Å] (5)	Dispersion [Å pixel ⁻¹] (6)
1	12–15	Jul	1999	CCD, LSS	325	3600–7800	4.6
2	12	Aug	1999	CCD, LSS	650	3700–6100	2.4
3	05–06	Sep	1999	CCD, LSS	650	3700–6100	2.4
4	01, 03	Nov	1999	CCD, LSS	325	3600–7800	4.6
5	27–30	Jul	2000	CCD, LSS	650	3700–6100	2.4
6	03–06	Oct	2000	CCD, LSS	650	3700–6100	2.4

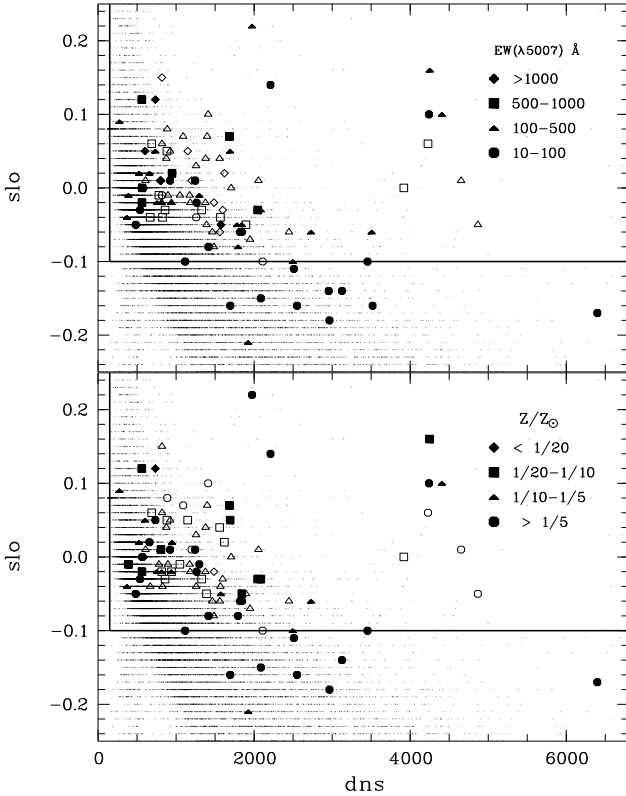


Fig. 2. *Top:* Positions of known galaxies from the training sample of BCGs from the SBS (filled symbols) and of BCGs from this paper (open symbols) in the plane of the two parameters characterizing the digitized low resolution prism spectra (LRS): the integral density (brightness) (dns) versus the slope of spectra (slo). This is to be compared to the parameters of objects of all types, as recorded from the HQS plates (dots plotted with the step of 0.01 on dns). Different symbols denote objects with different $EW([O\text{ III}]\lambda 5007)$ as indicated in the upper-right corner. *Bottom:* Same as above, but for galaxies with known metallicity. Different symbols denote galaxies with different metallicities. The rectangle indicates the final selection box (see text for details).

The choice of this limit is related to three facts. At first, all but one known BCGs with $Z \leq 1/20 Z_{\odot}$ have $EW([O\text{ III}]\lambda 5007) > 200 \text{ \AA}$. At second, in follow-up medium S/N spectra of faint galaxies, having the [O III]-line weaker than the limit indicated, the line [O III] $\lambda 4363 \text{ \AA}$ (which is 120 to ~ 40 times weaker than [O III] $\lambda 5007 \text{ \AA}$ for T_e in the range 12000 to 20000 K, Pagel et al. 1992), will be barely measurable, preventing a reliable determination of O/H. And at last, as shown by models of Schaerer & Vacca (1998), the decrease expected for the $H\beta$ equivalent widths after an instantaneous starburst is slower for lower metallicity models. For example, for $Z = 1/2.5 Z_{\odot}$ and $Z = 1/20 Z_{\odot}$ $EW(H\beta)$ decreases to a value of 50 \AA (roughly corresponding to $EW([O\text{ III}]\lambda 5007) \simeq 200 \text{ \AA}$, see Section 5 and Fig. 6) in 4.7 and 7 Myr, respectively. Suppose that we have an ensemble of BCG progenitors with a broad metallicity distribution. We suggest that these progenitors experience instantaneous starbursts with a quickly fading strength of emission lines. Then, due to the above effect, for the fixed threshold value of $EW(H\beta)$, the lower metallicity objects will be overrepresented in comparison to their real fraction among the progenitors. This additionally justifies the search for the most metal-deficient galaxies (with Z down to $1/50 Z_{\odot}$) among strong-lined BCGs.

In reality the situation is more complicated. The mean ratio of $I([O\text{ III}]\lambda 5007 \text{ \AA})/I(H\beta)$ (or equivalently, the ratio of their EWs, since these lines are rather close in wavelength) is a function of metallicity. It peaks near $Z \sim 1/10 Z_{\odot}$ at the level of $\sim 5 - 10$, as seen in the compilation and models of Stasinska & Leitherer (1996). For BCGs with $Z \sim (1/20 - 1/30) Z_{\odot}$ this ratio varies between ~ 2 and 6.5 (see, e.g., data in Skillman et al. 1988, Salzer et al. 1991, Izotov et al. 1994, van Zee et al. 1996, Kniazev et al. 1998, Thuan et al. 1999b, Kniazev et al. 2000a, 2000b, Fricke et al. 2001, and in this paper). For galaxies with Z as low as $\sim 1/40 - 1/50 Z_{\odot}$ it falls down to $\sim 1.5 - 3$ (see data for I Zw 18, SBS 0335–052 E and W, UGCA 292, e.g., in Izotov & Thuan 1999, Lipovetsky et al. 1999, van Zee 2000). For H II regions with metallicities near the solar value this ratio is usually found to be less than ~ 2 (e.g., van Zee et al. 1998c).

Therefore the threshold value of $\text{EW}([\text{O III}] \lambda 5007)$ of 200 Å for the extremely metal-deficient galaxies will correspond to a threshold in $\text{EW}(\text{H}\beta)$ of 50 – 130 Å, while for more typical BCGs this threshold in $\text{EW}(\text{H}\beta)$ will be only 35 – 40 Å. This will compensate, and even counteract (for the lowest metallicities we are seeking for, namely $Z \sim 1/50 Z_{\odot}$) the effect of a longer $\text{EW}(\text{H}\beta)$ decay, mentioned above. It is also useful to note that the primary selection criteria, which we impose for LRS, work against higher metallicity objects. In particular, as it is seen in the bottom panel of Figure 2, we miss about half of the BCGs with $Z > 1/5 Z_{\odot}$ but none of those with $Z < 1/10 Z_{\odot}$. All these factors should later be properly accounted for while the O/H distribution is analyzed with the aim to obtain an unbiased metallicity distribution.

Such strong-lined ELGs have a very low surface density. Thus, a sky region with an area of several thousand square degrees should be examined in order to end with a sample of the order of a hundred BCGs. It is crucial therefore to find the optimal region in the two-parameter space (slope (*slo*), density (*dns*)) used for automatic selection in the basic data-set of LRS spectra, to minimize the number of candidates, keeping at the same time the loss of strong-lined BCGs low. Based on the training BCG sample taken from the Second Byurakan Survey (see description of the sample in Ugryumov et al. 1999) we determine this region as follows (Fig. 2):

1. The LRS continua should be sufficiently blue, e.g. $slo \geq -0.1$.
2. The integrated density (roughly corresponding to the object brightness) should be sufficiently high, in order to minimize spurious “emission lines” due to noise peaks at low S/N, e.g. $dns \geq 150$.

The more stringent restriction of the “slope” parameter compared to the HSS $slo \geq -0.3$ allows us to avoid the region populated with lower excitation ELGs. This in turn leads to a large reduction in the number of spectra surviving this step of the selection procedure: the number of candidates decreases from 10 000 – 12 000 per plate in the HSS down to 2500 – 3500 per plate in the HSS-LM.

In contrast to the HSS an additional selection step using LRS data is therefore avoided. However, some strong-lined BCGs will then be missed and, after analysing the LRS parameters of ~ 100 strong-lined BCGs from the HSS and the SBS, we estimate this loss to be of the order 10 %. The next step of the selection procedure is performed by visual inspection of the high-resolution scans (HRS) of the candidates on a graphic display. Only candidates with really strong lines were selected.

Our experience from the HSS showed that galaxies with $\text{EW}([\text{O III}] \lambda 5007) > 150 - 200$ Å always show a strong signature in the high-resolution scans, making the interactive selection a non-critical step with respect to bias.

One of the advantages of the selection work performed for the HSS-LM is that for each field one HRS prism plate

has been fully digitized already with high resolution and is stored in a compact disk database. Therefore the time usually spent for rescanning individual spectra with high resolution was saved. On the other hand, there were some disadvantages related to the fact that only one (the best quality) prism plate per field was digitized with high resolution. This leads to a small number of emission-line candidates, in which the emission features are in fact artifacts, caused either by dust grains, or by possible ghosts or noise peaks. All such cases were detected in the course of applying additional selection procedures, as described below.

2.3. Additional selection with the use of the APM database and DSS-II images

The fainter candidates ($B \gtrsim 18^m0$) picked-up from the automatic selection procedure and visual inspection still contain many objects of unwanted types. In Fig. 3 we show how similar the HRS spectra of very different types of objects (BCG, QSO, blue star, M-star, AGN and absorption-line galaxy) can look.

Using the APM database (Irvin 1998) to separate star-like and extended objects as well as to get the APM ($B - R$) colour is quite helpful to reject further candidates. According to our previous experience with the selection of the HSS candidates, the great majority of APM star-like candidates with “strong emission” feature in the HRS near $\lambda 5000$ Å appeared to be either M-stars (in case of “red” APM colours ($B - R$) > 2), or quasars with $z \approx 3$ (in case of “neutral” APM colours ($B - R$) $\sim 1.0 - 1.7$) or B,A-stars with sufficiently strong H β absorption (in case of “blue” APM colours ($B - R$) < 1)).

“Blue” star-like objects have been checked additionally on the images of the Digitized Sky Survey (DSS-II) because some very compact BCGs could be hidden among them. All doubtful cases were kept in the list for follow-up spectroscopy at the 6 m telescope. In order to save observing time these objects were first observed with a short exposure ($\sim 1 - 3$ min) and only after confirmation of their true ELG nature a “normal” exposure (~ 20 min) was made.

One more category of non-BCG non-stellar strong-lined candidates was recognized with the help of the APM database and was removed from the observational list. These are APM “red” galaxies ($(B - R) > 1.7$), which from our earlier experience from the work with the HSS, and from cross-checking of our candidates with available spectra from the Sloan Digital Sky Survey Early Release Data (EDR) turned out to be either absorption-line galaxies with $z \sim 0.1$, or AGN type galaxies. A small number of strong-lined BCGs can occasionally appear in this range of $(B - R)$. From the statistics of HSS BCGs we estimate that we miss < 3 % of such objects.

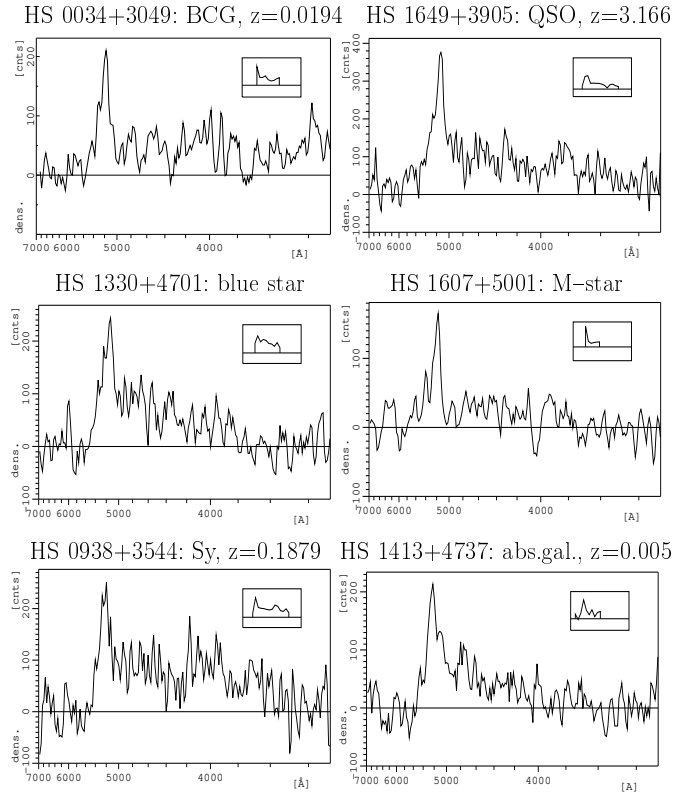


Fig. 3. Examples of faint HRS spectra selected as candidate strong-lined ELGs and their classification after follow-up spectroscopy: BCG, QSO, blue star, M-star, AGN and absorption-line galaxy.

3. Spectral observations and data reduction

3.1. The 6 m telescope spectroscopy

The results presented here were obtained from the observations with the Russian 6 m telescope during 6 runs between July 1999 and October 2000. The Long-Slit Spectrograph (LSS in Table 1; Afanasiev et al. 1995) attached to the telescope prime focus was used. Most of the long-slit spectra ($1''.2 - 2''.0 \times 120''$) were obtained with the grating of $651 \text{ grooves mm}^{-1}$, giving a dispersion of 2.4 Å pixel^{-1} . The data from the first and fourth runs were obtained with the grating of $325 \text{ grooves mm}^{-1}$ giving a dispersion of 4.6 Å pixel^{-1} . The scale along the slit was in both set-ups $0''.39 \text{ pixel}^{-1}$. For all observations the Photometrics CCD-detector PM1024 was used with a $24 \times 24 \mu\text{m}$ pixel size.

Normally, one or two exposures per object (10–20 minutes for one exposure depending on brightness and observational conditions) were used in order to detect the $[\text{O III}] \lambda 4363 \text{ Å}$ emission line and to measure the oxygen abundance by the classical standard method. Besides, for the most metal-deficient galaxies we got additional spectroscopy with higher S/N ratio, to confirm their very low metallicity. For about ten doubtful star-like candidates we got 1 – 3 min. exposure spectra to be sure we did not miss some very compact BCGs. For strong-lined galax-

ies the three strongest lines are well seen in such spectra. Reference spectra of an He–Ne–Ar lamp were recorded before or after each observation to provide the wavelength calibration. Spectrophotometric standard stars from Oke (1990) and Bohlin (1996) were observed for the flux calibration at least twice a night. All observations and data acquisition have been conducted under the NICE software package by Kniazev & Shergin (1995) in the MIDAS¹ environment.

All observations with exception of two nights were conducted during good photometrical conditions with a seeing of $1''.0 - 2''.0$. The two nights on August 12, 1999 and on July 29, 2000 (during which the spectra of 5 objects have been obtained) were non-photometrical, with the seeing of $3''.0 - 4''.0$. For two of them spectra of higher quality were acquired later in following runs.

3.2. Data reduction

The reduction of the spectra was performed at the SAO using the standard reduction systems MIDAS and IRAF².

Two-dimensional CCD images were automatically cleared from cosmic ray hits with the MIDAS routine FILTER/COSMIC. We then applied the IRAF package CCDRED to perform bad pixel removal, trimming, bias-dark subtraction, slit profile and flat-field corrections.

Prepared images were processed with the IRAF package LONGSLIT for wavelength calibration, distortion and tilt correction of each frame followed by sky subtraction and correction for atmospheric extinction. This standard way of reduction was performed by the routines: IDENTIFY, REIDENTIFY, FITCOORD, TRANSFORM, BACKGROUND and EXTINCTION.

To perform the flux calibration for all object images the instrumental response curves were obtained after the reduction of the spectrophotometric standard star spectra. This reduction includes as a first step, extraction of apertures of standard stars with the use of the APSUM procedure from the APEXTRACT package. In a second step STANDARD and SENSFUNC procedures transformed these apertures into sensitivity curves for the CALIBRATE procedure to perform flux calibration for all two-dimensional object images. To extract one-dimensional spectra from the flux calibrated images the APSUM routine was used. In case that more than one exposure was obtained with the same setup for an object, the extracted spectra were averaged.

For speeding-up and facilitating line measurements we employed command files created at the SAO using the FIT context and MIDAS command language. Their description was given in detail in Papers III-IV of the HSS.

¹ MIDAS is an acronym for the European Southern Observatory package — Munich Image Data Analysis System.

² IRAF is distributed by National Optical Astronomical Observatories, which is operated by the Association of Universities for Research in Astronomy, Inc., under cooperative agreement with the National Science Foundation

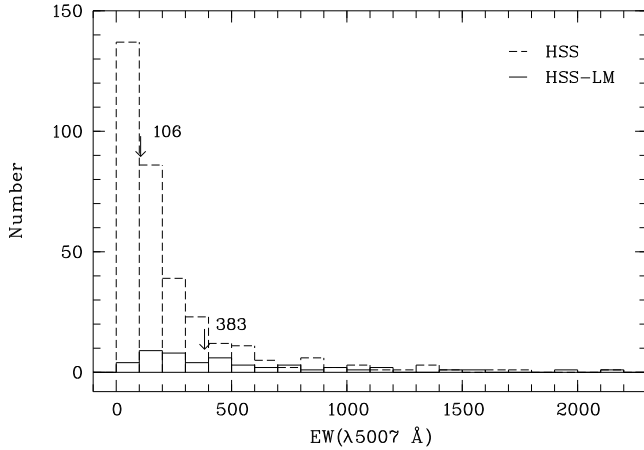


Fig. 4. The distribution of $EW([O\text{ III}]\lambda 5007)$ for all BCGs from this work (solid line) and similar data for all BCGs from the HSS (Paper I–V) (short dashed line). The arrows indicate median values. The number of ELG per bin in the HSS–LM increases, as expected, with the decrease of EW , reaching the maximum in the bin of $100 - 200\text{ Å}$ indicating that the completeness limit is in this range. For the HSS BCGs the number per bin grows till the last bin ($0 - 100\text{ Å}$). Since for the strong-lined BCGs/H II–galaxies a rather tight correlation exists between $EW([O\text{ III}]\lambda 5007)$ and $EW(H\beta)$ (see Fig. 6), we well pick up galaxies with $EW(H\beta) > 50\text{ Å}$. The latter limit corresponds to ages of instantaneous SF bursts of $T_{\text{burst}} < 4.7 - 7\text{ Myr}$ for the metallicity range of $1/20$ to $1/2.5 Z_{\odot}$ (Schaerer & Vacca 1998).

3.3. Oxygen abundances

The line fluxes were measured applying Gaussian fitting and integrating over the fitted profile with the INTEGRATE/LINE command under MIDAS. For blended lines, such as $H\alpha$, $[N\text{ II}]\lambda\lambda 6548, 6583\text{ Å}$, $[S\text{ II}]\lambda\lambda 6716, 6731\text{ Å}$ and $H\gamma$, $[O\text{ III}]\lambda 4363\text{ Å}$ a deblending procedure was used, assuming Gaussian profiles with the same FWHM as for single lines. The errors of the line intensities take into account the Poisson noise statistics and the noise statistics in the continuum near each line, and include uncertainties of data reduction. These errors have been propagated to calculate element abundances. For the simultaneous derivation of $C(H\beta)$ and $EW(\text{absorption})$, and to correct for extinction, we used the procedure described in detail by Izotov, Thuan & Lipovetsky (1994). The abundances of the ionized species and the total abundances of oxygen and other elements have been obtained following Izotov et al. (1994, 1997) and Izotov & Thuan (1999), which in turn are based on formulae from Aller (1984), and account for T_e differences in the zones with the predominant O^{++} and O^+ . In more detail the whole procedure is described in papers of Kniazev et al. (2000b) and Pustilnik et al. (2002a).

4. Results

We present here the data of 51 emission-line galaxies and one quasar which were observed in the frame of the HSS–LM in 1999–2000. 16 of these ELGs were already listed in the NED either as galaxies or as objects from various catalogs. For 12 of them NED presents radial velocities. For a few of these twelve galaxies there is also information in earlier publications on the presence of emission lines in their spectra, but there were no data on O/H except UGCA20. All these objects were included into our observing program as independently selected strong-lined candidates, expected to have a detectable $[O\text{ III}]\lambda 4363\text{ Å}$ line, and thus suitable for O/H determination. Comparison of our newly determined velocities (Table 2 and 3) with those for galaxies with already known redshifts shows a good consistency within the uncertainties given.

4.1. Emission-line galaxies

The results of the reduction and the galaxy spectra analysis are summarized in Tables 2 and 3. We give only integrated parameters of the galaxies studied, including the value of the oxygen abundance. For 24 of the galaxies presented various indications for characteristic WR features are detected. Of them 8 show a definite blue WR bump near $\lambda 4600 - 4700\text{ Å}$ only, another 7 show both blue and red ($\lambda 5800\text{ Å}$) WR bumps. 9 further ELGs show less confident WR blue bumps. This is consistent with the small ages of the SF bursts implied by their large values of EW of $H\beta$. The results of a more detailed analysis, including all observed line intensities and other heavy element abundances, as well as detailed information on the detected Wolf-Rayet features will be presented in forthcoming papers.

The strong-lined ELGs are listed in Table 2, while the ELGs with fainter lines ($EW([O\text{ III}]\lambda 5007) < 100\text{ Å}$) are separated in Table 3. Tables 2 and 3 contain the following information:

- column 1:* The object’s IAU-type name with the prefix HS.
- column 2:* Right ascension for equinox J2000.
- column 3:* Declination for equinox J2000. The coordinates were measured on direct plates of the HQS and are accurate to $\sim 2''$ (Hagen et al. 1995).
- column 4:* Heliocentric velocity in km s^{-1} .
- column 5:* r.m.s. of the heliocentric velocity uncertainty in km s^{-1} .
- column 6:* Blue apparent magnitudes based on the values from the APM database. The latter were corrected following Kniazev et al. (2002) to transfer them to the Johnson *B*-band system. Their r.m.s. uncertainty is estimated as $0^m.45$.
- column 7:* The extinction A_B in our Galaxy in the *B*-band, (Schlegel et al. 1998).
- column 8:* The absolute *B*-magnitudes are calculated from the apparent ones in *column 6* and the heliocentric velocities and are corrected for A_B in *column 7*.
- columns 9,10:* The equivalent widths of the emission lines

$H\beta$ and $[O III] \lambda 5007$ in Ångström.

column 11 (Table 2): The derived values of $12+\log(O/H)$. Their r.m.s. uncertainties vary from 0.02 dex for the largest S/N of the $[O III] \lambda 4363$ Å line to ~ 0.2 dex for the lowest S/N (see plots of the spectra in Appendix A). The most uncertain data (~ 0.2 dex) are marked by a colon.

column 12 (Table 2) and *column 11* (Table 3): One or more alternative names, according to information from NED. Reference numbers are given to other sources for redshift-spectral information indicating that a galaxy is an ELG.

According to our spectral classification all, but two of the observed ELGs turned out to be BCGs with a characteristic HII-region spectrum and low luminosity. The only exceptions are the two galaxies HS 2300+2612 and HS 0053+2910. The former is classified as Starburst Nucleus (SBN), the latter – as Dwarf Amorphous Nucleus Starburst (DANS). The classification criteria applied follow those of Salzer (1989a). Here Salzer’s classes SS, DIIH and HIIH are taken together as one class of blue compact/HII galaxies (BCG) (see also Ugryumov et al. 1999).

The spectra of all emission-line galaxies are shown in Appendix A, which is available only in the electronic version of the journal.

Since for part of the observed galaxies the $[O III] \lambda 4363$ Å line was only barely detected and the derived O/H value is of low precision, we have checked these objects with the empirical strong-line method devised by Pilyugin (2000, 2001), giving an independent estimate. In all cases but one we got consistent results within the cited uncertainties. The one exclusion is HS 2259+2357, for which we have an estimate of $12+\log(O/H)=8.0 \pm 0.2$, while Pilyugin’s method gives 8.6.

4.2. UGCA 20

This galaxy was selected under the name HS 0140+1943 as a candidate strong-lined object. In the process of cross-check it was identified in NED as the galaxy UGCA 20, for which high S/N spectroscopy was obtained by van Zee et al. (1996). From the high S/N spectra of its two identified HII regions they determined an oxygen abundance of $12+\log(O/H)=7.58 \pm 0.03$. Our detailed study of this galaxy (a paper in preparation) resulted in an even lower metallicity: $12+\log(O/H)=7.42 \pm 0.06$.

4.3. Quasar HS 0057+2049

This new faint ($m_B=18^m7$) quasar was observed as a “blue” star-like candidate (see the end of Section 2) to a possible very compact BCG. Its coordinates are $\alpha_{2000}=01^h00^m27^s.7$, $\delta_{2000}=+21^\circ05'42''$. The strong and broad emission line at $\lambda \approx 4980$ Å is unambiguously identified with Ly α , what gives a redshift of 3.0983 ± 0.0004 . The

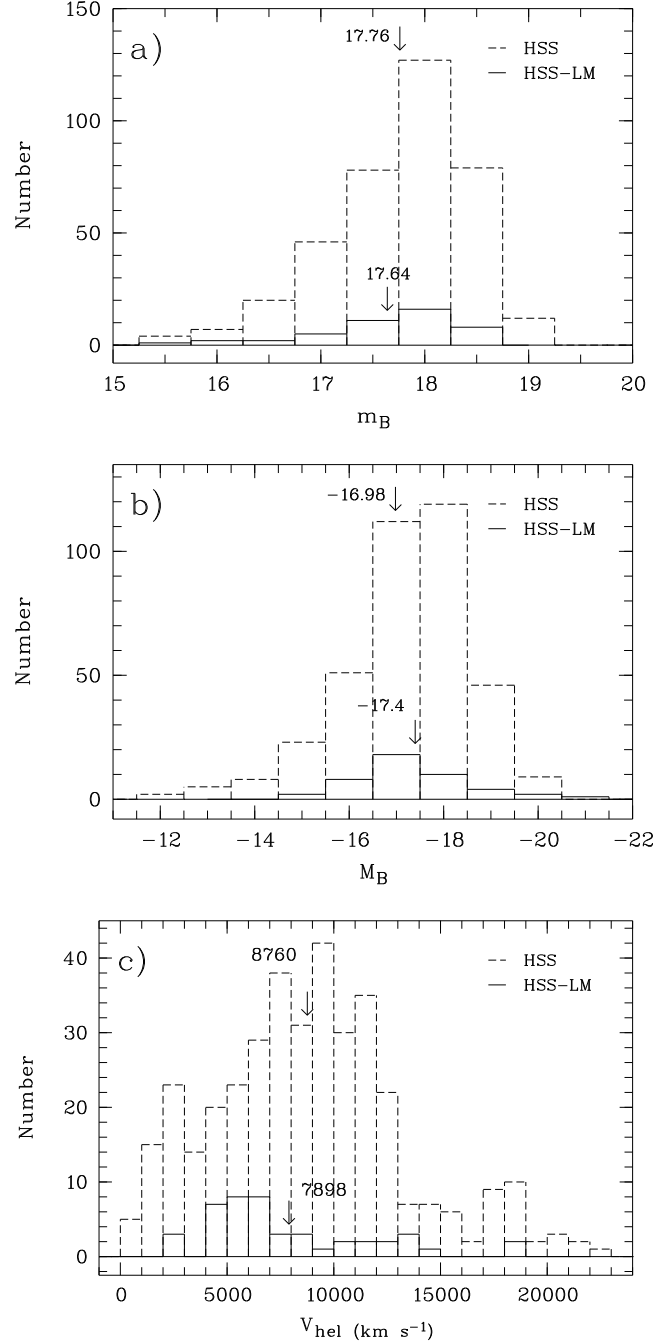


Fig. 5. Distributions of apparent (a), and absolute (b) B -magnitudes and of V_{hel} (c) for the sample of HSS-LM BCGs with $EW([O III] \lambda 5007) \geq 100$ Å in comparison to all BCGs from the HSS (Paper I–V). The arrows indicate mean values. The Figures show the trend of these low-mass galaxies to be well sampled up to $m_B \sim 18$ and $V_{hel} \sim 7000$ km s $^{-1}$.

finding chart of this quasar and the plot of its spectrum can be found on the www-site of the Hamburg Quasar Survey (<http://www.hs.uni-hamburg.de/hqs.html>).

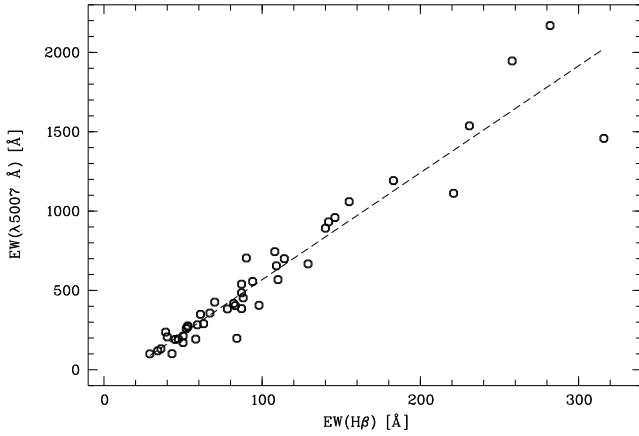


Fig. 6. The observed relation between the $EW([O\text{ III}]\lambda 5007)$ and $EW(H\beta)$ of 46 strong-lined BCGs from Table 2. The dashed line is a linear fit to the data. The threshold value of $EW([O\text{ III}]\lambda 5007) = 200\text{ \AA}$ for the expected completeness limit of the sample corresponds to $EW(H\beta) = 50\text{ \AA}$.

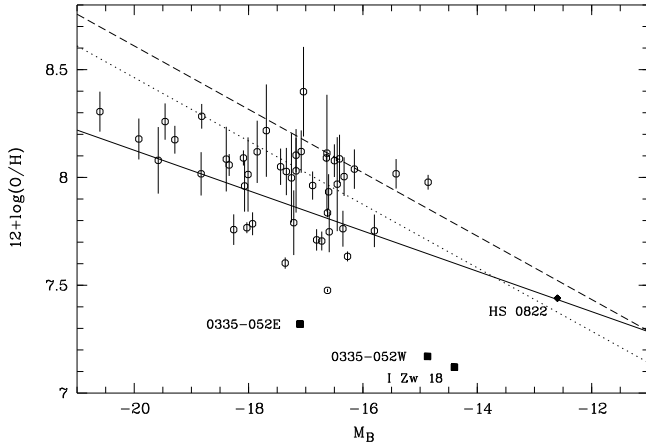


Fig. 7. The strong-lined BCGs (open circles) from Table 2 plotted in the well known diagram metallicity vs blue luminosity (e.g. Skillman et al. 1989), originally shown for dwarf irregular galaxies. The dashed line shows the original relation found by Skillman et al. (1989), the dotted line shows that relation shifted to the left by 1^m to account for the expected brightening of BCGs. The solid line is a linear fit to our observed data with the weights accounting for O/H uncertainties. The error bars of O/H correspond to $\pm 1\sigma$. Pay attention that three of the most metal-deficient BCGs (not taken for the estimate of this linear fit), shown by filled squares, strongly deviate from any of the fitting lines.

5. Discussion and conclusions

5.1. Current results and relation to the goals

We have presented above the description of the new project and its first results. The extremely low-metallicity

galaxies are very rare objects, and the discovery of a few such objects, probably does not well justify the efforts undertaken. Therefore, another important goal of the project is to create a large BCG sample with reliably measured O/H and a well defined selection function.

The first goal of the project is shown to be reached given the discovered galaxies with O/H lower than $1/20$ of the solar value. Three such very rare objects were discovered, and one more was rediscovered. We expect that among the remaining candidates a comparable number of extremely metal-poor galaxies will be found. Thus, HSS-LM will substantially increase the whole number of these unusual objects, and will advance the study of their population properties and the search for truly young local dwarf galaxies.

As for the second goal the results presented above allow to formulate some preliminary conclusions and to estimate its perspectives.

First, the selection procedures elaborated, based on the Hamburg Quasar Survey LRS and HRS databases, supplemented by information from the APM database and DSS II images, yields a very high fraction of strong-lined BCGs. Namely, 37 ELGs with $EW([O\text{ III}]\lambda 5007) \geq 200\text{ \AA}$ out of 52 observed candidates (that is 71 %) have been found (see also Fig. 4). This confirms the high efficiency of the applied selection method.

Second, a preliminary analysis of the parameters of the new strong-lined BCGs (see Fig. 5), indicates reasonable completeness of the sample with well determined O/H in apparent B -magnitude up to $\sim 18^m$. The distribution of the sample BCGs in radial velocity is increasing up to $V_{\text{hel}} = 7000\text{ km s}^{-1}$. This implies that all BCGs with $M_B \leq -17^m0$ will be picked up with high efficiency. Based on the HSS experience, the well sampled velocity range is probably larger.

Third, the temperature-sensitive weak line $[O\text{ III}]\lambda 4363\text{ \AA}$ was detected in 43 BCGs in a sky region covering $\sim 1/3$ of the entire HSS-LM area. The oxygen abundances $12 + \log(O/H)$ derived for these BCGs vary in the wide range between ~ 7.4 and 8.4 , having a typical uncertainty of ~ 0.1 dex. The number of homogeneously selected BCGs with reliable O/H value expected in the whole sky zone of the HSS-LM is $\gtrsim 100 - 120$ galaxies. They will provide a good opportunity to make first steps toward the understanding a selection-free metallicity distribution of the local gas-rich galaxies — BCG progenitors.

5.2. New sample and its relation to BCGs from the HSS

The comparison of parameters of the observed BCG subsample from the HSS-LM with those for BCGs from the HSS (Fig. 5) shows that the latter are distributed rather similar to the former in apparent blue magnitude B , in absolute M_B and in radial velocity. Their mean values are quite close: $\langle B \rangle = 17^m64$ and 17^m76 ,

$< M_B > = -17^m40$ and -16^m98 , and $< V_{\text{hel}} > = 7898$ and 8760 km s^{-1} for the HSS-LM and the HSS respectively. Therefore we expect that the well selected sample of strong-lined BCGs from HSS-LM can be combined with the subsample of about one hundred strong-lined BCGs in the HSS zone to derive a metallicity distribution.

5.3. Preliminary results on parameter correlations

To illustrate statistical relations between BCG parameters discussed in this paper and in the literature we show Figures 6 and 7 based on the data obtained here in this paper.

In Fig. 6 we present a rather tight relation between the EW s of $H\beta$ and $[O III] \lambda 5007 \text{ \AA}$. This correlation allows to fix the ages of instantaneous SF bursts, which are well picked up by the applied selection criterion based on the $EW([O III] \lambda 5007)$ (see Introduction).

The other important relation is often discussed for dIrr galaxies: there is a general trend of metallicity decrease with decrease of blue luminosity (e.g. Skillman et al. 1989, Richer & McCall 1995). For BCGs, if they are related to other gas-rich low-mass galaxies, one could expect a similar relation. Current data, presented in Fig. 7, show a rather large scatter, so it is difficult to draw definite conclusions from the strong-lined BCG data available. The overall trend seen in the data fits however well with previous results (c.f. Kunth & Östlin (2000); their Fig. 10). It is worth to note however, that the extremely metal-deficient BCGs strongly deviate from any relation valid for the rest of the BCGs. This implies that the search for the most metal-poor BCGs should not be concentrated on the least luminous candidates only.

Summarizing the presented results, we draw the following conclusions:

1. The HSS-LM is a new HQS based project, which very efficiently samples the strong-lined ELGs of H II/BCG type. After the 6 m telescope follow-up spectroscopy 71 % of the candidates (37 galaxies) were found to be BCG/H II-galaxies with $EW([O III] \lambda 5007)$ in the range of 200 to 2100 Å.
2. Among these galaxies 3 new very metal-deficient BCGs were found with Z in the range $1/28$ to $1/20 Z_{\odot}$. One more such galaxy – UGCA 20 – with $Z = 1/35 Z_{\odot}$ was rediscovered as one of the HSS-LM targets.
3. For 43 strong-lined BCGs the oxygen abundance was determined with the use of the temperature sensitive faint line $[O III] \lambda 4363 \text{ \AA}$. Its full range corresponds to ionized gas metallicities between $1/28$ and $1/3 Z_{\odot}$.

This paper presents about 1/3 of the galaxies from the final sample of strong-lined BCGs of this survey. The observations of the remaining objects are expected to be completed during the years 2002 – 2003.

Acknowledgements. A.V.U. is very grateful to the staff of the Hamburg Observatory for their hospitality and kind assistance. We acknowledge the partial support from INTAS (grant

97-0033), Russian state program “Astronomy” and Center of Cosmoparticle Physics “Cosmion”. The authors are thankful to the referee G.Östlin for useful suggestions. This research has made use of the NASA/IPAC Extragalactic Database (NED) which is operated by the Jet Propulsion Laboratory, California Institute of Technology, under contract with the National Aeronautics and Space Administration. The use of the Digitized Sky Survey (DSS-II) and APM Database is gratefully acknowledged.

References

- Afanasiev, V. L., Burenkov, A. N., Vlasjuk, V. V., & Drabek, S. V. 1995, SAO RAS internal report No. 234
- Aller, L. H. 1984, *Physics of Thermal Gaseous Nebulae*, Dordrecht: Reidel
- Aloisi, A., Tosi, M., & Greggio, L. 1999, *AJ*, 118, 302
- Bergvall, N., Rönback, J., Masegosa, J., & Östlin, G. 1999, *A&A*, 341, 697
- Bohlin, R. C. 1996, *AJ*, 111, 1743
- Campos-Aguilar, A., Moles, M., & Masegosa, J. 1993, *AJ*, 106, 1784
- Doublier, V., Comte, G., Petrosian, A., et al. 1997, *A&AS*, 124, 405
- Eder, J. A., Oemler, A. J., Schombert, J. M., & Dekel, A. 1989, *ApJ*, 340, 29
- Fairall, A. 1998, *Large-Scale Structures in the Universe*, Wiley-Praxis series in astronomy and astrophysics, Wiley, New York
- Fricke, K. J., Izotov, Y. I., Papaderos, P., Guseva, N. G., & Thuan, T. X. 2001, *AJ*, 121, 169
- Hagen, H.-J., Groote, D., Engels, D., & Reimers, D. 1995, *A&AS*, 111, 195
- Haro, G. 1956, *Bol Obs. Tonantzintla y Tacubaya*, 2, 8
- Hopp, U., & Kuhn, B. 1995, in *Reviews in Modern Astronomy*, ed. G. Klare, 8, 277
- Hopp U., Engels D., Green, R., et al. 2000, *A&AS*, 142, 417 (HSS-III)
- Irwin, M. 1998, <http://www.ast.cam.ac.uk/~apmcat/>
- Izotov, Y. I., & Thuan, T. X. 1999, *ApJ*, 511, 639
- Izotov, Y. I., Lipovetsky, V. A., Guseva, N. G., Kniazev A. Y., & Stepanian, J. A. 1993, in *DAEC Workshop, The Feedback of Chemical Evolution on the Stellar Content of Galaxies*, eds. D. Alloin, & G. Stasinska, Meudon Obs., 127
- Izotov, Y. I., Thuan, T. X., & Lipovetsky, V. A. 1994, *ApJ*, 435, 647
- Izotov, Y. I., Thuan, T. X., & Lipovetsky, V. A. 1997, *ApJS*, 108, 1
- Izotov, Y. I., et al. 2002, in preparation
- Izotov, Y. I., Chaffee, F. H., Foltz, C. B., et al. 2001, *ApJ*, 560, 222
- Kniazev, A. Y., & Shergin, V. S. 1995, SAO RAS internal report No. 249, 1
- Kniazev, A. Y., Pustilnik, S. A., & Ugryumov, A. V. 1998, *Bulletin SAO*, 46, 23
- Kniazev, A. Y., Pustilnik, S. A., Ugryumov, A. V., & Kniazeva, T. F., 2000a, *Astronomy Lett.*, 26, 163
- Kniazev, A. Y., Pustilnik, S. A., Masegosa, J., et al. 2000b, *A&A*, 357, 101
- Kniazev, A. Y., Engels D., Pustilnik, S. A., et al. 2001, *A&A*, 366, 771 (HSS-IV)
- Kniazev, A. Y., Pustilnik, S. A., Ugryumov, A. V., et al. 2002, in preparation

- Kunth, D., & Östlin, G. 2000, *A&AR*, 10, 1
- Kunth, D., Maurogordato, S., & Vigroux, L. 1988, *A&A*, 204, 10
- Legrand, F., Tenorio-Tagle, G., Silich, S., Kunth, D., & Serviño, M. 2002, *AJ*, in press = astro-ph/0106431
- Leitherer, C., Schaerer, D., Goldader, J. D., et al. 1999, *ApJS*, 123, 3
- Lipovetsky, V. A., Chaffee, F. H., Izotov, Y. I., et al. 1999, *ApJ*, 519, 177
- Lu, N. Y., Hoffman, G. L., Groff, T., Roos, T., & Lamphier, C. 1993, *ApJS*, 88, 383
- MacAlpine, G. M., Smith, S. B., & Lewis, D. W. 1977, *ApJS*, 34, 95
- Mac Low, M.-M., & Ferrara, A. 1999, *ApJ*, 513, 142
- Mamon G. A. 1999, in ASP Conference Series Cosmic Flows: Towards an Understanding of the Large-Scale Structure of the Universe, eds. S. Courteau, M. Strauss, & J. Willick, in press
- Markarian, B. E. 1967, *Afz*, 3, 55
- Markarian, B. E., Lipovetsky, V. A., & Stepanian, J. A. 1983, *Afz*, 19, 29
- Masegosa, J., Moles, M., & Campos-Aguilar, A. 1994, *ApJ*, 420, 576
- Mouri, H., & Taniguchi, Y. 2000, *ApJ*, 545, L103
- Oke, J. B. 1990, *AJ*, 99, 1621
- Östlin, G., 2000, *ApJ*, 535, L99
- Östlin, G., & Kunth, D. 2001, *A&A*, 371, 429
- Östlin, G., Amram, P., Bergvall, N., Masegosa, J., Boulesteix, J., & Márquez, I. 2001, *A&A*, 374, 800
- Pagel, B. E. J., Simonson, E. A., Terlevich, R. J., & Edmunds, M. G. 1992, *MNRAS*, 255, 325
- Papaderos, P., Izotov, Y. I., Fricke, K. J., Thuan, T. X., & Guseva, N. G. 1998, *A&A*, 338, 43
- Papaderos, P., Izotov, Y. I., Thuan, T. X., et al. 2002, *A&A*, submitted = astro-ph/0207314
- Pesch, P., Stephenson, C. B., & MacConnell, D. J. 1995, *ApJS*, 98, 41
- Pilyugin, L. 2000, *A&A*, 362, 325
- Pilyugin, L. 2001, *A&A*, 369, 594
- Popescu, C. C., Hopp, U., Hagen, H.-J., & Elsässer, H. 1996, *A&AS*, 116, 43
- Popescu, C. C., Hopp, U., Hagen, H.-J., & Elsässer, H. 1998, *A&AS*, 133, 13
- Pustilnik, S. A., Ugryumov, A. V., Lipovetsky, V. A., Thuan, T. X., & Guseva, N. G. 1995, *ApJ*, 443, 499
- Pustilnik, S. A., Engels, D., Ugryumov, A. V., et al. 1999, *A&AS*, 137, 299 (**HSS-II**)
- Pustilnik, S. A., Brinks, E., Thuan, T. X., Lipovetsky, V. A., & Izotov, Y. I. 2001a, *AJ*, 121, 1413
- Pustilnik, S. A., Kniazev, A. Y., Lipovetsky, V. A., & Ugryumov, A. V. 2001b, *A&A*, 373, 24
- Pustilnik, S. A., Kniazev, A. Y., Masegosa, J., et al. 2002a, *A&A*, 389, 779
- Pustilnik, S. A., Kniazev, A. Y., Pramsky, A. G., Ugryumov, A. V., & Masegosa, J. 2002b, *A&A*, submitted
- Pustilnik, S. A., Engels, D., Masegosa, J., et al. 2002c, *A&A*, in preparation (**HSS-VI**)
- Richer, M. G., & McCall, M. L. 1995, *ApJ*, 445, 642
- Salzer, J. J. 1989a, *ApJ*, 347, 152
- Salzer, J. J., & Norton, S. A. 1999, in ASP Conference Series 170, Proc. of IAU colloq., Low Surface Brightness Universe, eds. J. I. Davies, C. Impey, & S. Phillipps, 253
- Salzer, J. J., McAlpine, G. M., & Boroson T. A. 1989b, *ApJS*, 70, 447
- Salzer, J. J., Di Serego Alighieri, S., Matteucci, F., Giovanelli, R., & Haynes, M. P. 1991, *AJ*, 101, 1258
- Salzer, J. J., Moody, J. W., Rosenberg, J. L., Gregory, S. A., & Newberry, M. V. 1995, *AJ*, 109, 2376
- Sargent, W. L. W., & Searle, L. 1970, *ApJ*, 162, L155
- Schaerer, D., & Vacca, W. D. 1998, *ApJ*, 497, 618
- Schaerer, D., Contini, T., Kunth D., & Meynet G. 1997, *ApJ*, 481, L75
- Schaerer, D., Contini, T., & Kunth D. 1999, *A&A*, 341, 399
- Searle, L., & Sargent, W. L. W. 1972, *ApJ*, 173, 25
- Schlegel, D., Finkbeiner, D. P., & Douglas, M. 1998, *ApJ*, 500, 525
- Schulte-Ladbeck, R. E., Hopp, U., Greggio, L., & Crone, M. 2000, *AJ*, 120, 1713
- Silich, S., & Tenorio-Tagle, G. 2001, *ApJ*, 552, 91
- Skillman, E., Melnick, J., Terlevich, R., & Moles, M. 1988, *A&A*, 196, 31
- Skillman, E., Kennicutt, R., & Hodge, P. 1989, *ApJ*, 347, 875
- Stasinska, G., & Leitherer, C. 1996, *ApJS*, 107, 661
- Stasinska, G., Schaerer, D., & Leitherer, C. 2001, *A&A*, 370, 1
- Stepanian, J. A. 1994, Proc. IAU Symp. 161, Kluwer, Dordrecht, eds. H. T. MacGillivray, et al., 731
- Taylor, C. L., Brinks, E., Grashuis, R. M., & Skillman, E. D. 1995, *ApJS*, 99, 427
- Telles, E., & Terlevich, R. 1997, *MNRAS*, 286, 183
- Terlevich, R., Melnick, J., Masegosa, J., Moles, M., & Copetti, M. V. F. 1991, *A&AS*, 91, 285
- Thuan, T. X., Izotov, Y. I., & Lipovetsky, V. A. 1995, *ApJ*, 445, 108
- Thuan, T. X., Lipovetsky, V. A., Martin, J.-M., & Pustilnik, S. A. 1999a, *A&AS*, 139, 1
- Thuan, T. X., Izotov, Y. I., & Foltz, C. B. 1999b, *ApJ*, 525, 105
- Thuan, T. X., Izotov, Y. I., Foltz, C. 2000, *ApJ*, 525, 105
- Ugryumov, A. V., Pustilnik, S. A., Lipovetsky, V. A., Richter, G. M., & Izotov, Y. I. 1998, *A&AS*, 131, 285
- Ugryumov, A. V., Engels, D., Lipovetsky, V. A., et al. 1999, *A&AS*, 135, 511 (**HSS-I**)
- Ugryumov, A. V., Engels, D., Kniazev, A. Y., et al. 2001, *A&A*, 374, 907 (**HSS-V**)
- Vilchez, J. M. 1995, *AJ*, 110, 1090
- York, D. G., Adelman, J., Anderson, J. E., et al. 2000, *AJ*, 120, 1579
- van Zee, L., 2000, *ApJ*, 543, L31
- van Zee, L., Haynes, M. P., Salzer, J., & Broelis, A. 1996, *AJ*, 112, 129
- van Zee, L., Skillman, E. D., & Salzer, J. J. 1998a, *AJ*, 116, 1186
- van Zee, L., Westpfahl, D., Haynes, M., & Salzer, J. 1998b, *AJ*, 115, 1000
- van Zee, L., Salzer, J. J., Haynes, M. P., O'Donoghue, A. A., Balonek, T. J. 1998c, *AJ*, 116, 2805
- Zenina, O. A., Balinskaya, I. S., Kniazev, A. Y., & Lipovetsky, V. A. 1997, *Astronomy Reports*, 41, 472
- Zwicky, F. 1966, *ApJ*, 143, 192

Table 2. Parameters of the strong-lined BCGs

#	Name	α (2000)	δ (2000)	V_{hel}^a (km s ⁻¹)	$\pm\sigma_V$ (km s ⁻¹)	m_B^b	A_B^c	M_B^d	$EW_{H\beta}$ (Å)	$EW_{\lambda 5007}$ (Å)	12+log(O/H) ^e	Other names from NED and number of reference (12)
	(1)	(2)	(3)	(4)	(5)	(6)	(7)	(8)	(9)	(10)	(11)	(12)
1	HS 0017+1055	00 20 21.4	+11 12 21	5650	± 12	18.26	0.15	-16.27	146	959	7.63	[SS98] 84, 1
2	HS 0024+2314	00 26 52.4	+23 31 13	6967	± 10	17.51	0.10	-17.44	40	207	8.04	
3	HS 0029+1443	00 32 18.5	+15 00 11	5325	± 17	17.52	0.15	-16.88	87	485	7.96	1
4	HS 0029+1748	00 32 03.2	+18 04 44	2188	± 30	17.62	0.15	-14.86	183	1192	7.97	NPM1G +17.0024, 1
5	HS 0031+2645	00 34 19.7	+27 02 09	4105	± 12	18.07	0.15	-15.80	53	270	7.75	
6	HS 0034+3047	00 37 36.8	+31 04 08	5825	± 45	18.22	0.19	-16.45	50	212	7.96:	
7	HS 0041+2333	00 44 20.5	+23 50 00	6554	± 24	16.76	0.11	-18.07	61	349	7.96	[SS98] 88, 1
8	HS 0044+3052	00 47 26.9	+31 09 02	5209	± 13	17.77	0.16	-16.63	50	171	8.11:	
9	HS 0048+2744	00 51 05.9	+28 00 35	6974	± 10	17.71	0.19	-17.34	70	426	8.02	
10	HS 0051+2812	00 54 23.5	+28 29 09	18490	± 12	17.83	0.15	-19.29	78	383	8.17	
11	HS 0052+2536	00 54 56.4	+25 53 08	13606	± 15	16.85	0.13	-19.58	34	119	8.07:	IRAS F00522+2537
12	HS 0052+2537	00 54 56.0	+25 53 23	13737	± 12	18.44	0.13	-18.01	82	418	8.01	IRAS F00522+2537
13	HS 0058+1847	01 01 32.3	+19 03 33	11192	± 19	18.10	0.08	-17.85	59	283	8.11	1
14	HS 0103+3219	01 06 03.6	+32 35 32	5341	± 10	18.31	0.17	-16.15	83	404	8.03	
15	HS 0109+3304	01 12 30.6	+33 20 04	4846	± 10	17.74	0.16	-16.50	67	357	8.07	KUG 0109+330
16	HS 0111+2115	01 14 37.6	+21 31 16	9445	± 12	16.14	0.10	-19.46	110	568	8.25	NPM1G +21.0056, 1
17	HS 0113+1750	01 16 40.3	+18 05 51	18756	± 21	18.25	0.08	-18.82	155	1059	8.28	1
18	HS 0119+3059	01 22 14.6	+31 15 16	4793	± 27	17.64	0.19	-16.60	87	539	7.93	
19	HS 0121+1753	01 24 00.0	+18 09 04	7760	± 12	18.01	0.11	-17.17	52	260	8.10	
20	HS 0122+0743	01 25 34.2	+07 59 22	2922	± 10	15.68	0.14	-17.36	221	1112	7.60	UGC 00993, 2
21	HS 0123+1624	01 26 17.3	+16 40 29	8720	± 10	17.12	0.14	-18.34	94	556	8.05	1
22	HS 0127+2706	01 29 47.0	+27 22 20	12566	± 12	15.75	0.23	-20.60	98	406	8.30	
23	HS 0128+2832	01 31 21.3	+28 48 12	4833	± 36	17.62	0.20	-16.64	258	1946	8.09	
24	HS 0131+1649	01 33 59.1	+17 04 44	11124	± 12	17.17	0.15	-18.83	63	290	8.01	
25	HS 0134+3415	01 37 13.8	+34 31 12	5800	± 30	17.95	0.11	-16.62	282	2169	7.83	
26	HS 0137+2935	01 40 24.1	+29 51 05	4669	± 48	17.33	0.15	-16.81	129	667	7.71	
27	HS 0137+3152	01 40 41.8	+32 07 19	8039	± 12	18.12	0.17	-17.21	29	100	7.79:	
28	HS 0140+1943	01 40 30.3	+19 43 47	574	± 20	15.78	0.06	-13.56	73	246	7.42	UGCA 20, 3
29	HS 0143+2400	01 45 54.4	+24 15 55	10350	± 19	18.00	0.33	-18.03	140	892	7.76	1
30	HS 0205+3212	02 08 28.1	+32 27 05	5044	± 15	18.10	0.28	-16.33	90	704	8.00	
31	HS 0248+2001	02 51 06.8	+20 13 42	6402	± 18	17.95	0.39	-17.08	45	191	8.12	
32	HS 2236+1344	22 38 31.1	+14 00 29	6183	± 12	18.15	0.17	-16.62	316	1458	7.47	
33	HS 2252+1752	22 55 15.3	+18 08 35	12747	± 33	16.48	0.24	-19.92	87	385	8.17	
34	HS 2252+2032	22 55 11.6	+20 48 48	13764	± 12	18.58	0.18	-17.93	142	932	7.78	
35	HS 2256+2610	22 58 57.2	+26 26 23	7833	± 39	17.61	0.18	-17.69	84	198	8.21:	IRAS F22565+2610, 2MASXi J2258572+262623
36	HS 2258+2046	23 00 32.2	+21 02 30	5588	± 19	18.02	0.22	-16.59	88	453	7.74	
37	HS 2258+2215	23 00 43.2	+22 31 13	10629	± 39	17.55	0.17	-18.39	36	132	8.08:	
38	HS 2259+2357	23 01 38.0	+24 14 05	7791	± 12	18.04	0.18	-17.25	43	101	8.00:	
39	HS 2304+2255	23 07 18.9	+23 11 54	6293	± 10	17.75	0.27	-17.17	114	700	8.03:	
40	HS 2311+2631	23 13 48.0	+26 48 02	6008	± 60	18.34	0.20	-16.41	39	237	8.08	
41	HS 2336+1800	23 38 46.8	+18 17 20	4991	± 12	17.48	0.07	-16.72	58	193	7.70	
42	HS 2340+2034	23 42 38.2	+20 51 31	2260	± 21	17.16	0.14	-15.42	108	744	8.01	
43	HS 2347+1618	23 50 06.0	+16 35 06	14731	± 30	18.29	0.08	-18.26	109	655	7.75	
44	HS 2348+2920	23 50 50.4	+29 37 03	4822	± 17	17.91	0.18	-16.35	47	194	7.76	
45	HS 2352+2733	23 54 56.7	+27 49 59	8285	± 12	18.29	0.09	-17.04	53	276	8.40:	
46	HS 2359+1659	00 02 09.9	+17 15 59	6275	± 30	16.59	0.06	-18.09	231	1537	8.09	

^a Heliocentric velocities; ^b corrected APM magnitudes (Kniazev et al. 2002); ^c extinction estimates from NED following Schlegel et al. (1998);

^d absolute magnitudes are corrected for galactic extinction; ^e less confident values are denoted by a colon

References: **1** – Popescu et al. 1996; **2** – Lu et al. 1993; **3** – van Zee et al. 1996

Table 3. Parameters of Emission-Line Galaxies with $EW_{\lambda 5007} < 100\text{\AA}$.

#	Name	α (2000)	δ (2000)	V_{hel}^a (km s ⁻¹)	$\pm\sigma_V$ (km s ⁻¹)	m_B^b	A_B^c	M_B^d	$EW_{\text{H}\beta}$ (\AA)	$EW_{\lambda 5007}$ (\AA)	Other names from NED and number of reference (11)
	(1)	(2)	(3)	(4)	(5)	(6)	(7)	(8)	(9)	(10)	
1	HS 0001+1703	00 04 11.7	+17 19 49	5478	± 99	17.79	0.07	-16.61	5	31	
2	HS 0053+2910	00 56 27.6	+29 27 10	11041	± 100	17.00	0.20	-19.05	–	–	NPM1G +29.0035, 2MASXi J0056275+29271
3	HS 2300+2612	23 03 20.2	+26 28 52	23803	± 87	17.20	0.20	-20.52	17	25	
4	HS 2319+2723	23 21 41.9	+27 39 48	5936	± 69	17.86	0.25	-16.92	–	22	ESDO F535-09, LEDA 141110, [HR89] 231913.4+272316, 4
5	HS 2336+2112	23 38 32.2	+21 28 41	5619	± 111	17.05	0.09	-17.43	16	82	

^a heliocentric velocities; ^b corrected APM magnitudes (Kniazev et al. 2001); ^c extinction estimates from NED following Schlegel et al. (1998);

^d absolute magnitudes are corrected for galactic extinction

References: **4** – Eder et al. 1989

Appendix A: Spectra of emission-line galaxies from the HSS-LM